RFID-Based Indoor Positioning Using Edge Machine Learning

Massimo Merenda, *Member, IEEE*, Luca Catarinucci, *Senior Member, IEEE*, Riccardo Colella, *Senior Member, IEEE*, Demetrio Iero, Francesco G. Della Corte, *Senior Member, IEEE*, and Riccardo Carotenuto, *Senior Member, IEEE*

***Abstract*—Indoor positioning of objects and people is becoming of great importance in the Internet of Things (IoT), in-home automation, and navigation in malls, airports, or very large buildings. Positioning is determined by multiple distance measurements between reference points and sensors. Distance measurement uses the time of flight of an ultrasonic signal traveling from an emitter to receiving sensors. This requires close synchronization between the emitter and the sensors and a sharp time resolution of the time of arrival (TOA) of the ultrasonic signal. Usually, TOA is detected using cross-correlation processing requiring significant computational resources at the sensors level. In this work, the synchronization is done using the RFID standard protocol features. The TOA detection is performed firstly by training off-line a Machine Learning model using as input the peaks indexes of the ultrasonic signal received and the output of a cross-correlation based positioning system, as ground-truth. In a second phase, the positioning is evaluated and tested on-board using the previously trained model on a microcontroller. The system architecture is presented and experimental results on the positioning accuracy are shown accordingly. Results show a mean positioning error below 25 cm in 95% of the positionings in a typical room.**

***Index Terms*—Indoor ultrasonic positioning, RFID synchronization, RFID tag, edge machine learning.**

I. Introduction

EMERGING technologies such as indoor navigation, asset tracking, and personal advertising require the provision of accurate indoor positioning systems (IPS) [1]. In recent years, IPS have already proven to be suitable for many of these applications providing position information with sufficient accuracy at an affordable price [2], [3].

They can be used profitably for augmented and virtual reality gestural interfaces [4]–[8], for indoor navigation [9], [10], for medical rehabilitation [11], [12] and recognition of human posture, for monitoring position and activity of elderly and disabled people [13], plant monitoring [14], aided manufacturing [15], and security [16].

Typically, the positioning of a mobile unit or sensor is calculated in two steps: 1) the distances of the mobile unit from a number of fixed reference points (RP) are measured; 2) these distances are used to geometrically determine the position of the sensor in the given reference system [17].

One of the most widely used methods of deriving the sensor position from the emitter-sensor distances is trilateration or multilateration in the case of multiple distance measurements. Multilateration uses the distances between RP and the point to be located as radii of spheres, at the intersection of which the position searched for is located. In 3D space, four is the minimum number of spheres, and therefore of RP, but this is reduced to three if only one half-space is to be used for positioning.

In recent years, it has been shown that the required distances can be measured with high accuracy and at a reasonable cost using ultrasonic traveling waves [18], [19]. From the knowledge of the speed of sound in the air, it is possible to estimate the distance from the travel time, i.e., the Time of Flight (TOF), from the emitter to the receiver. Precisely, the TOF is the time elapsed from the instant when a signal is emitted (time of emission, TOE) to the instant of its arrival (time of arrival, TOA) at the receiver, i.e., TOF = TOA - TOE. Therefore, a close synchronization between the local clocks of the transmitter and receiver is required to achieve accurate distance measurements. Several synchronization techniques have been proposed in the literature [20], [21].

To estimate TOF, the TOA must first be estimated. Cross-correlation is a commonly adopted technique for accurate and reliable TOA estimation; it measures the similitude of transmitted and received signals as a function of the temporal offset of one to the other. The relative displacement, or lag, that produces the maximum value is proportional to the TOA, provided the TOE is known. By its integral nature, cross-correlation shows a reduced sensitivity to disturbances by exploiting all the information contained in the signals [22].

Among the different techniques available [23], one of the most performant is that based on the linear chirp, which is a sinusoidal signal that linearly shifts the frequency from a lower frequency up to a higher frequency over a fixed time

Manuscript received 1 March 2022; revised 11 May 2022; accepted 1 June 2022. Date of publication 16 June 2022; date of current version 23 September 2022. *(Corresponding author: Massimo Merenda.)*

Massimo Merenda is with the Center for Digital Safety and Security, AIT Austrian Institute of Technology GmbH, 1210 Vienna, Austria (e-mail: massimo.merenda@ait.ac.at).

Luca Catarinucci and Riccardo Colella are with the Department of Innovation Engineering, University of Salento, 73100 Lecce, Italy (e-mail: luca.catarinucci@unisalento.it; riccardo.colella@unisalento.it).

Demetrio Iero and Riccardo Carotenuto are with the DIIES Department, University Mediterranea of Reggio Calabria, 89124 Reggio Calabria, Italy (e-mail: demetrio.iero@unirc.it; r.carotenuto@unirc.it).

Francesco G. Della Corte is with the DIETI Department, University of Napoli Federico II, 80125 Naples, Italy (e-mail: francescogiuseppe.dellacorte@unina.it).

Digital Object Identifier 10.1109/JRFID.2022.3182819

interval, since the chirp auto-correlation shows a very sharp and easily recognizable peak [24], [25].

According to the survey of Machine Learning (ML) techniques used for indoor positioning presented in [10], the adaptation of ML-based solutions in indoor localization is still in its infancy. To our knowledge, the problem of synchronization when using ultrasound signals for indoor positioning has not been previously addressed with ML techniques so far.

In this work, we consider an innovative positioning system that, instead of having an RF link between emitter and sensors for synchronization, uses the features of the RFID protocol standard. In particular, we exploit as the synchronization signal the standard tag hardware function that detects the presence of an RF event, as presented in [26]. An RFID tag is included in the ultrasound emission subsystem and each sensor. When the RFID reader irradiates its interrogation pulse, all tags receive it at the same time with small uncertainty. This way, emitters and receivers start their operations at the same time. Moreover, we avoid the need to explicitly calculate the cross-correlation, applying an ML algorithm to infer in a single step the positioning coordinates. This leads to a reduction of the overall computational burden on the device.

This approach provides benefits in terms of the number of electronic components to be used, not requiring additional circuitry for synchronization or a devoted infrastructure for the broadcasting of synchronization messages. Nevertheless, we achieve reduced computational effort and power consumption.

Moreover, in this work, we extend the results previously presented in [26]. The main addition to the previous work consists of the TOA detection directly performed at a microcontroller level exploiting Edge Machine Learning (EML) technique. Firstly, we trained off-line a Machine Learning (ML) algorithm exploiting a Multi-Output Regressor (MOR) model, using as input the peaks' indexes of the raw ultrasonic signal received and as desired ground-truth output the coordinates produced by a cross-correlation based positioning system. In a second phase, the positioning is evaluated and tested on-board using the previously trained model on a microcontroller. The system architecture is presented and experimental results on the positioning accuracy are shown accordingly, also considering possible perturbations on the synchronization accuracy from the RFID infrastructure. Calculations ensure a mean positioning error below 25 cm in the 95% of the positioning frames, in the volume of a typical room.

By obtaining the coordinates locally, the user memory of the RFID tag can be further exploited for saving the position coordinates, updating their content after each positioning frame, allowing the dual use of the RFID infrastructure both for synchronization and for the transport layer of positioning data.

The paper is structured as follows: Section II describes the system architecture and its operation, while Section III reports the experimental results and their discussion. Finally, Section IV draws the conclusions of the paper.

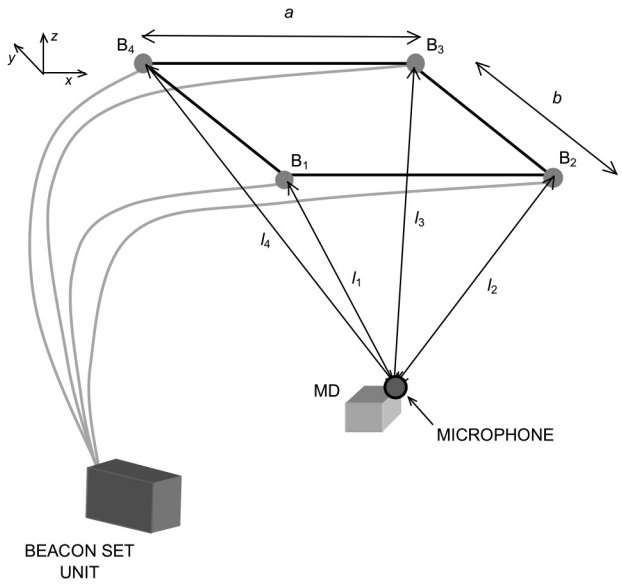

Fig. 1. System architecture. The Beacon Set Unit emits the ultrasonic chirp signals through the four beacons B_1, B_2, ...B_4; the microphone records the four ultrasonic signals. An external PC calculates the MD position.

II. System Architecture and Operation

A novel system for indoor sensors' positioning using a synchronization mechanism based on RFID technology and EML positioning, is presented.

Specifically, the RFID technology provides emitter-sensor synchronization, and EML computes sensors' positioning, without performing cross-correlation.

A laboratory-level positioning system [21] provides the ultrasonic signal data and the related frame by frame sensor positions.

From the ultrasonic record of each positioning frame, are extracted four significant features, namely the time occurrence of the signal peak of each of the four time-slots in which is naturally divided the received ultrasonic signal. The said four features are the inputs while the desired output is the triad of coordinates (x, y, z) of the microphone in the given positioning frame.

The laboratory positioning system is briefly explained, followed by the description of the EML.

The ultrasonic system architecture consists of a PC, a Data Emission/Acquisition board, a set of ultrasonic emitters, and a wired microphone. It emulates the system and is capable of executing the synchronous positioning described in detail in [17]. Briefly, the system described in [17] gives the position of the microphone using a sphere intersection technique based on four TOFs that are calculated employing synchronized emissions and reception ultrasonic signals via a suitable RF channel.

By positioning four RPs coplanar to the vertices of a square of side a (see Fig. 1), the system of intersections of the four spheres can be written as follows:

$$\begin{cases} l_{1j}^2 = x^2 + y^2 + z^2 \\ l_{2j}^2 = (x-a)^2 + y^2 + z^2 \\ l_{3j}^2 = (x-a)^2 + (y-b)^2 + z^2 \\ l_{4j}^2 = x^2 + (y-b)^2 + z^2 \end{cases} \quad (1)$$

The solution of the system composed of the first, second, and third equations of the (1) can be written in closed form:

$$x_1 = \frac{l_{1j}^2 - l_{2j}^2 + a^2}{2a}$$
$$y_1 = \frac{l_{1j}^2 - l_{4j}^2 + b^2}{2b}$$
$$z_1 = \sqrt{\left| l_{1j}^2 - x_1^2 - y_1^2 \right|}. \quad (2)$$

The rectangular placement of RPs produces a closed-form solution of the intersection of the spheres using only three of them. Choosing in all combinations three equations at a time from the four from (1) yields four sets of coordinates for the position of the target microphone. The results are averaged to make them more robust against small and unbiased errors on the four distance estimates:

$$\begin{cases} x = \frac{1}{4}\sum_{h=1}^{4} X_h \\ y = \frac{1}{4}\sum_{h=1}^{4} y_h \\ z = \frac{1}{4}\sum_{h=1}^{4} z_h \end{cases} \quad (3)$$

The location mechanism integrates a mechanism to identify and discard any incorrect distance estimates that would result in an incorrect calculation of the sensor position. In fact, each equation continues to output coordinates for the target even when one or more distance measurements are incorrect, thus providing wrong positions.

For this aim, the Euclidean distance D between the four computed sensor positions using (4) is calculated as the square root of the sum of squared differences between every pair of coordinates out of the four calculated coordinate sets:

$$D = \sqrt{\sum_{\substack{h,k=1 \\ k>h}}^{4} (X_h - X_k)^2 + \sum_{\substack{h,k=1 \\ k>h}}^{4} (y_h - y_k)^2 + \sum_{\substack{h,k=1 \\ k>h}}^{4} (Z_h - Z_k)^2}. \quad (4)$$

D represents the sum of the distances between the six combinations of two out of the four points generated by the four sets of equations derived from (1). If one or more distance measurements are incorrect, D is greater than a given threshold, and the calculated current position is considered incorrect and thus discarded.

Operations start with the four beacons emitting the ultrasonic signals in a preset sequence (i.e., 1, 2, 3, 4, $T_{SILENCE}$, 1, 2, 3, 4 $\cdots$) starting at the externally triggered time $t_{0BEACONS}$. Each emitting period is $T_{EMISSION}$. The beacons belong to the same circuit and are inherently synchronized with each other. The signals sequence is repeated at regular time intervals of duration T_{FRAME} (frame repetition time). The ultrasonic signal is a chirp that allows maximum exploitation of correlation during ranging.

Starting from time $t_{0BEACONS}$ the microphone records the ultrasonic signal coming from the emitters for a duration time of T_{FRAME}, in accordance with its default setting. Next, the PC cross-correlates the recorded signal with a stored template signal, computes four TOAs, and estimates the four distances from time $t_{0BEACONS}$. Subsequently, the microphone position is calculated using multilateration.

As previously introduced, in previous works [17], [21] we used cross-correlation to achieve high accuracy results, however, in this work we aim at using EML techniques to directly estimate the positioning coordinates.

The external trigger or emission start time $t_{0BEACONS}$, is usually stated according to the Broadcast-Reference Synchronization, one of the most reliable synchronization techniques [27]. This technique concerns a sender broadcasting a message to a multitude of receivers who receive the message at the same time. With this approach, the synchronization is among the receivers, which all receive the message at the same time, but not between sender and receivers.

In [26] has been demonstrated that a Synchronization technique that relies on the exploitation of the features of the RFID protocol standard through an RFID reader, using a tag hardware function that detects the presence of an RF event, is suitable for achieving comparable results. Experimental tests have assessed an average uncertainty of about 10 ms and a maximum uncertainty of about 30 ms at a distance up to 3.6 m from the RFID reader. Under reasonable assumptions, the mean ranging error is 3-4 mm while the maximum error is limited to 12 mm. In presence of such ranging errors, the error propagation analysis shows that an overall mean positioning accuracy of about 4-5 centimeters can be achieved while, in the worst case, the positioning error is limited to 15 cm.

In our case, the Beacon Unit and the sensor are equipped with an RFID tag arranged to have an output pin that indicates when the tag detects the standard RFID reading beacon.

The beacon unit and the sensors are both irradiated by the same RFID reader, and therefore receive at the same time the interrogation beam, which starts the received interrogation beam to the emitting process in the Beacon Unit and the recording process in the sensor. In this manner, they are closely synchronized with each other only with a certain time interval of uncertainty, or time jitter.

III. Experimental Setup and Discussion

This section presents the setup of the experiment for estimating the positioning error using the EML method, and the obtained results are shown and discussed.

Setup: The prototype emulates the positioning system [17] and shows the same positioning performances. It emits the same signals, performs the same data operations, and produces the same positioning results as the system shown in [17].

The positioning is computed by feeding the time location of the four peaks in the recorded received signal track to the EML trained model. Subsequently, by comparing the positions obtained independently with the two approaches, synchronous and EML, the incremental error occurring with the presented EML method is evaluated.

In the PC/Board system, there is no synchronization jitter since the emitting and receiving phases of the ultrasonic signal are inherently synchronous as they are handled by the Data Emission/Acquisition board processor itself. Accordingly, a uniformly random time shift has been added to the position

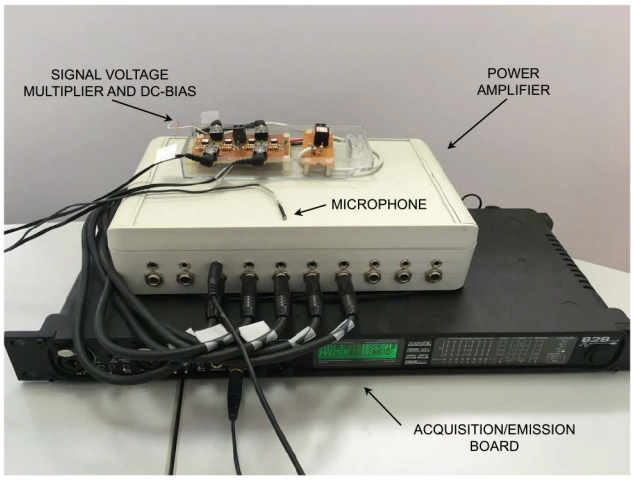

Fig. 2. Data emission/acquisition board, power amplifier, signal voltage multiplier, 200 V DC-bias circuitry, and microphone.

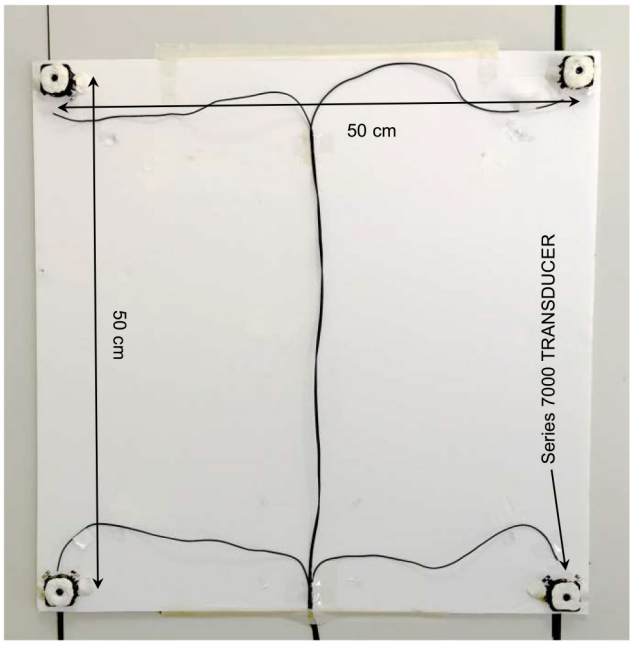

Fig. 3. Beacon Set Unit, consisting of a panel of size 52 ' 52 cm^2 containing four ultrasonic SensComp Series 7000 transducers. Their emission cone half-angle (far-field) is widened from 24.7 up to 80.95° at 50 kHz by reducing the aperture diameter to 8.5 mm.

calculation to emulate the RFID synch uncertainty that impacts the real-world system.

The positioning system setup includes the following components:

– Processing unit: a personal computer is used to execute a MATLAB program that generates the ultrasonic signal and acquires, stores, and analyses the signals from the single microphone mimicking the position sensor.

– Data Emission/Acquisition Board: four outputs and one input of a MOTU 828 mk3 audio interface, connected with the PC through a FireWire port, are used. A linear up-chirp signal in the bandwidth 30-50 kHz is used; it is composed of 512 samples at 192 kSamples/s, and a Hanning window is applied to avoid audible "clicking".

– Ultrasonic power amplifier and emitters: the generated signals are emitted in sequence through the four MOTU outputs, and then amplified with a four-channel Class AB MOSFET power amplifier. Each channel is further raised to 300 Vp-p with a voltage multiplier made using the 1:100 coil transformer Coilcraft LPR6235-752S, and then fed to four ultrasonic SensComp Series 7000 electrostatic transducers [28]. The capacitive transducers are DC-biased at 200 V provided by the EMCO Q02-5-R DC-DC converter.

The four transducers are placed at the corners of a 50 × 50 cm2 square, and placed on a panel with the face towards the room volume (see Fig. 3). The used transducers were adapted as already reported in [17] since they were not conceived for this application and their emission cone is too narrow to cover the entire intended volume. Their half-angle of emission cone (far-field) was enlarged from 24.7° to 80.95° at 50 kHz by reducing the aperture diameter to 8.5 mm with a proper mask.

– Mobile Device (MD): it is emulated by a miniature microphone, sampled by the MOTU board at 192 kSamples/s. The microphone is a micromachined condenser microphone by Knowles Acoustics FG-6163, enclosed in a cylindrical package with 2.6 mm length and diameter, and a 0.79 mm acoustical receiver window diameter, already used in [17].

Note that, in the presented experimental setup, the emitted signal is a chirp, which is used by the system to calculate the ground-truth position of the microphone using cross-correlation. However, the best signal for the technique based on the identification of the position of the peaks is the pulse-shaped one, as narrow as possible. Therefore, a better result can be expected from the EML technique using an *ad hoc* signal.

EML training and validation (Dataset): The dataset was collected using the hardware system described in the previous section.

Multiple measurements were recorded while moving the microphone in a standard office room. Each measurement, or record, corresponds to a time duration of T_{FRAME}, and a tuple of coordinates (x, y, z).

Every single record has 8705 features, representing the intensity of the received ultrasonic signal acquired from the MOTU hardware. A software routine exploits a cross-correlation based algorithm [17] to calculate the ground-truth positioning coordinates (x, y, z), for each record.

The whole information of a single measurement is then obtained, comprising 8705 features + 3 coordinates, resulting in 8708 values record length. From the ultrasonic record of each positioning frame, four significant features are extracted, namely the time of the signal peak occurrence within each of the four timeslots in which is naturally divided the received ultrasonic signal. The said four input features are saved in a new vector of 4 features per record, while the desired output is the coordinates triplet (x, y, z) of the microphone in the given positioning frame.

After the process of feature selection, the whole information of a single acquisition, or positioning frame, is then reduced to the size of 4 features + 3 coordinates, resulting in a record

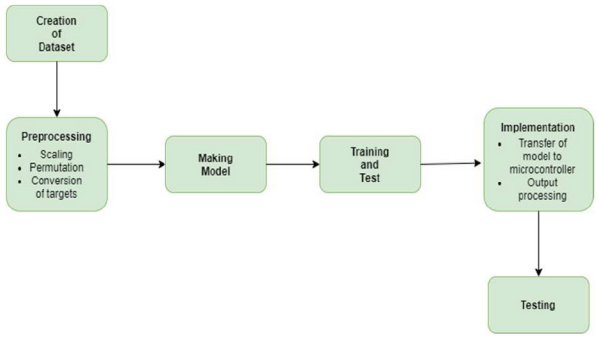

Fig. 4. Block Diagram of the MLOps process.

length of 7 values. The process is repeated for all the carried-out positioning frames (2828).

It is worthwhile noting that the process to select the four peaks indexes can be easily obtained in real-time using a microcontroller along with the acquisition of the signal from the ultrasonic microphone, reducing the burden of post-processing and the requirements in terms of required memory and latency.

For convenience, the data was preprocessed in MATLAB and exported in CSV format for subsequent processing in Python.

Algorithm: The phases of the presented algorithm, shown in Fig. 4, are:

– *Dataset creation*, explained in the previous paragraph.

– *Data preprocessing,* consisting of a number of steps to organize the data in order to improve the training process of the model.

– *Model making*, consisting in generating the model by selecting the optimal solutions for the specific application.

– *Training and test*, consisting in training the model and evaluating its effectiveness in outputting the required accuracy.

– *Implementation*, consisting of: i) transferring the model to the microcontroller; ii) microcontroller the microcontroller firmware for real-time data capture and pre-processing; iii) feeding input data to the model; iv) post-processing of the data generated by the model.

– *Testing*, consisting in testing the performance of the whole system. Performance is analyzed in terms of both accuracy and speed of execution.

The preprocessing phase was performed using the Python language on JupiterLab.

Input features of the dataset were scaled with the StandardScaler to normalize the range of features in the data. The dataset values were split into inputs and targets and divided into training (80%), testing (10%), and validation (10%).

Attention must be paid to the overfitting problem that could produce a model that learns training values with overly high accuracy, degrading performance when new inputs other than those used for training are used. To prevent overfitting, the indices of the vectors holding the scaled values are permutated.

Model: Multi-output regressions (MOR) are regression problems that involve the prediction of two or more numeric values given different input values. MOR requires special machine learning algorithms that output multiple variables for each input record.

The choice of ML algorithms is based on several motivations, according to the nature of the problem (classification, regression). In our approach, we mainly considered performance, complexity, dataset size, training time and cost, inference time and final size of the model. Main goal was to concurrently obtain good values of training and inference speed and accuracy, which are the most important parameters taken into account with this edge computing implementation. MOR methods enable effective modeling of multi-output datasets by considering not only the underlying relationships between features and their corresponding targets, but also the relationships between the targets, resulting in a more accurate representation and interpretability of real-world problems; also, these techniques have the advantage of producing simpler models with higher computational efficiency [29]. Deep learning neural networks are an example of a method that supports multi-output regression natively, providing a good accuracy also with small dataset with a reduced number of features, acceptable training times. Moreover, they provide reduced inference time when compared to tree-based models and other more performant algorithms that, however, show limitations when embedded in resource-constrained hardware devices.

In this work, we designed a neural network model leveraging the Keras deep learning library, basically parallelizing three regression models that consist of an input layer, a dense layer, and an output layer with linear activation. This model was trained for 500 epochs, with a batch size of 10, using the Adam optimizer.

Microcontroller: The aim of the system in this work is to estimate the positioning of an MD by applying a multi-output regressor model to the time occurrence, i.e., the record index, of the signal peak of each of the four time-slots in which is naturally subdivided the recorded ultrasonic signal of a single positioning frame. For the purpose of this work, these features have been extracted in a post-processing phase.

As already stated, the process to select the indexes can be easily carried out in real-time using a microcontroller during the acquisition of the signal from the ultrasonic microphone, with a reduced post-processing burden, latency, and required memory. Due to this reason, we used the STWIN SensorTile wireless node (STEVAL-STWINKT1B), a development kit that simplifies prototyping and testing of advanced industrial IoT applications. The kit consists of a core system board with an ultra-low-power microcontroller and some embedded sensors for applications including analysis of vibration of 9 degrees of freedom motion sensing data, high-frequency audio and ultrasound investigation, and precision temperature control. The microcontroller deployment was carried out using STM32CubeIDE software by STMicroelectronics, with the Artificial Intelligence pack X-CUBE-AI. Subsequently, a neural network based on the Keras model was deployed and evaluated.

RFID Tag: For the purpose of realizing a proof of concept of the integrated solution, we took into account the characteristics of the well-known tag EM4325 [30] The programmable

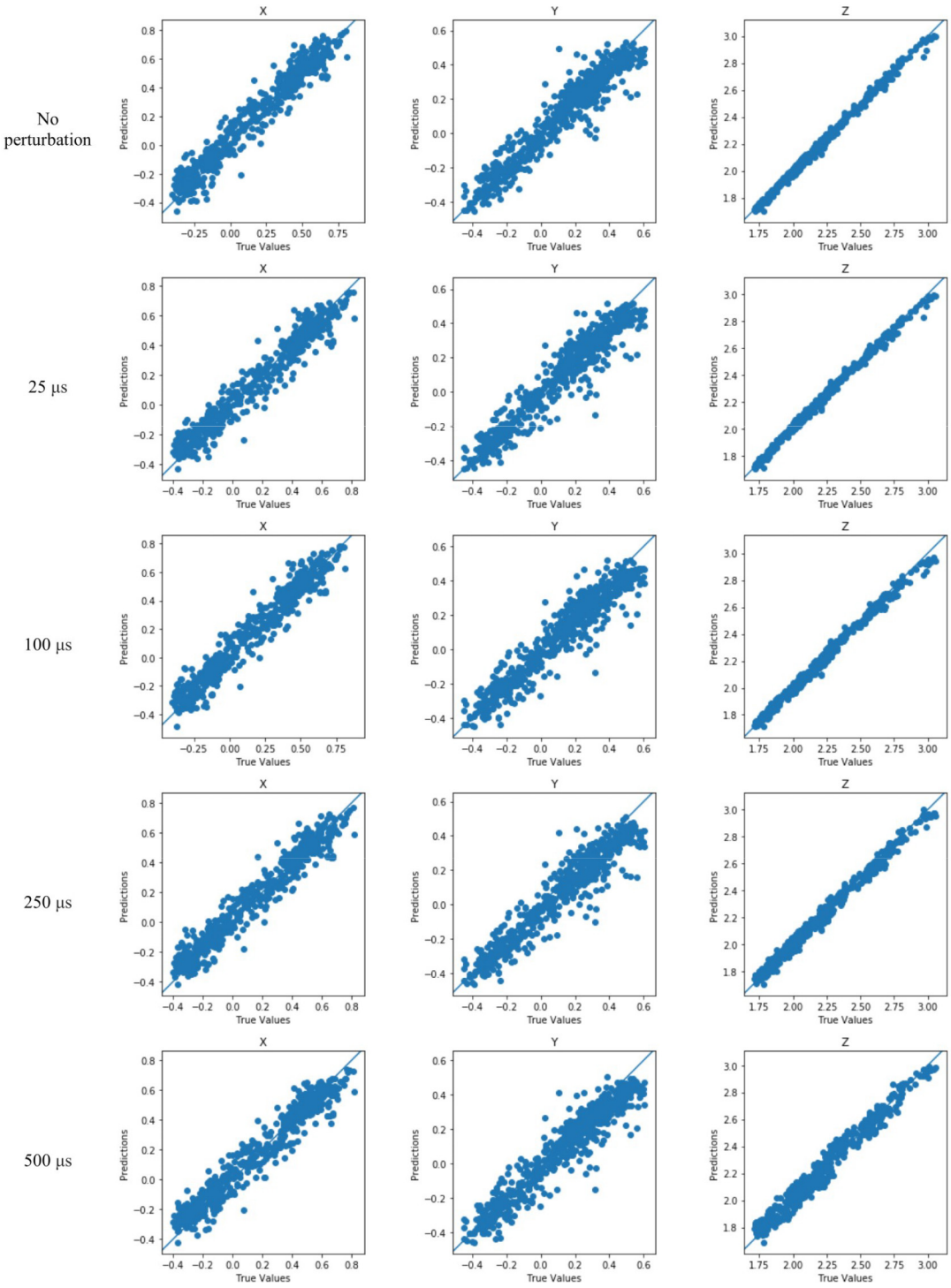

Fig. 5. Effect of perturbation on ML model accuracy. The predicted coordinates are compared to the actual ground-truth values while perturbating the original dataset (from 0 to 500 μs), thus mimicking the effect of unstable jitter due to timing synchronization issues exploiting the RFID infrastructure.

external interfaces could be used as Serial Peripheral Interface (SPI) bus, allowing the EM4325 to function as an RF front end and protocol handler in advanced RFID tags or embedded applications. In [26], we exploited the standard tag hardware function of EM4325 that detects the presence of an RF event as the synchronization signal. In this work, we also analyzed the effect of the writing on the tag user position on the overall performance and characteristics of the positioning system.

The writing on the tag user memory of the coordinates accounts for a tenth of milliseconds, nor introducing relevant additional delay or limiting the positioning rate of the single device. It is worth nothing that the number of devices does not have any effect on the overall accuracy of the system,

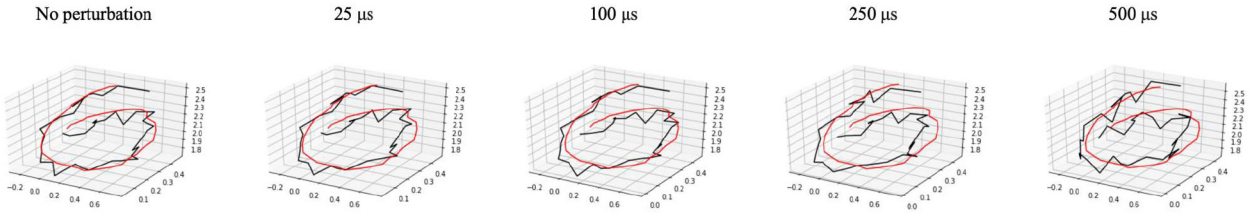

Fig. 6. Trajectories comparison.

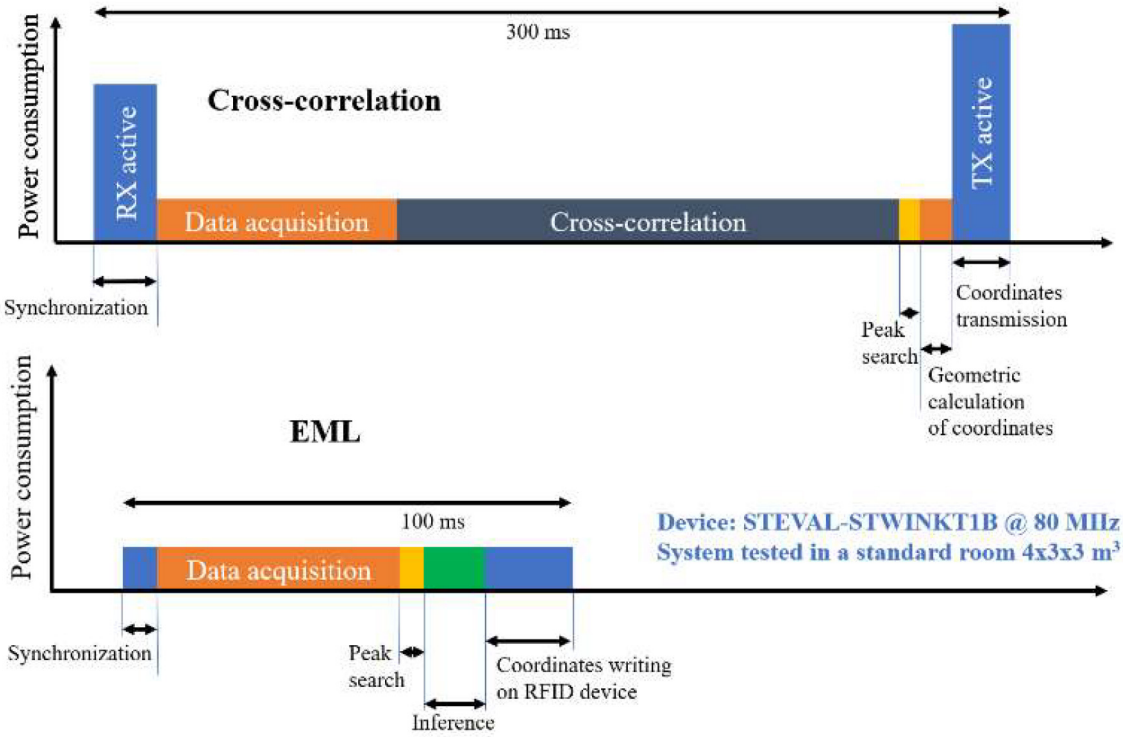

Fig. 7. Conventional cross-correlation-based times and power consumption compared with the proposed EML system (not in scale).

due to the fact that the coordinates are inferenced locally on each device. Nevertheless, the frequency of positioning can be affected by an increasing number of devices that indeed require longer times for the reading of the coordinates saved in each tag's user memory. It does depend on many concurrent factors, among them the specific reader protocol used, the number of devices identified for each research query, antenna's gain for both reader and tag, etc.

Results: The results are shown in Figs. 5 and 6. The predicted coordinates are compared to the actual ground-truth values while perturbating the original dataset, thus mimicking the effect of unstable jitter due to timing synchronization issues exploiting the RFID infrastructure. The results show that the accuracy of prediction degrades with the increase of the perturbation values (from 0 to 500 μs).

In Fig. 6, the trajectory is reconstructed for perturbation values from 0 to 500 μs and compared to the trajectory calculated using the cross-correlation technique.

Fig. 7 shows the Cumulative Distribution Function (CDF) of the positioning error. It is confirmed that, also in the worst case, positioning accuracy of 25 cm is achievable in 95% of the positionings.

Comparison between cross-correlation and EML positioning: Although there are many systems for ultrasonic positioning, we consider the comparison between the proposed RFID-based EML system and one of the most accurate, cross-correlation-based, conventional system [17]. The conventional system generates the (x, y, z) positioning coordinates by performing several steps.

First, the transmitter and receiver are synchronized via an RF signal. Second, the receiver records the acoustic signal in a time window related to the maximum distance to be reached (e.g., 4.37 m in a 4 m x 4 m x 3 m room), recording samples in a total time window of 17.9 ms, including the duration of the emitted chirp signal. This is done for the four signals thus requiring four times longer listening window (71.6 ms) for a total of 13747 samples. This step is also performed in the proposed EML system.

A moving-window cross-correlation of 512 samples with the template signal is performed on this signal, for a total of about 7 M sum and addition operations, which required in the conventional system [17] about 1/3 s each individual placement.

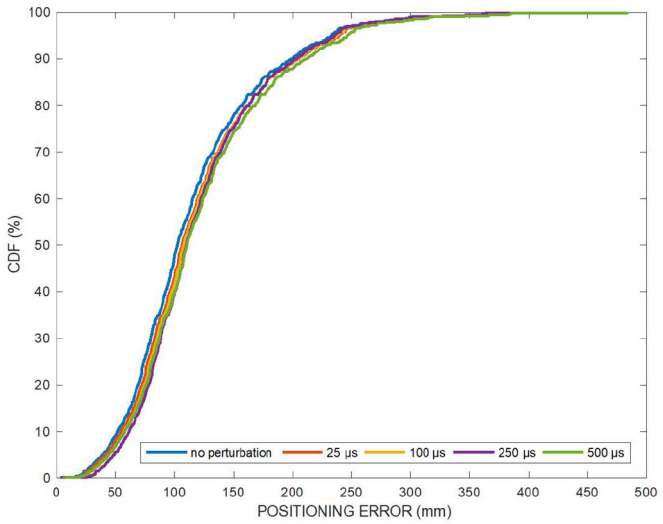

Fig. 8. Cumulative Distribution Function (CDF), or percentage of readings with an error lower than the given abscissa value, of the EML positioning error.

Then, the four peaks corresponding to the four ToFs are detected (this is also done in the proposed EML system). From the four peaks, the four beacon-sensor distances are made, considering the actual speed of sound in the air.

The geometric calculation of the sensor coordinates is then performed from the four distances.

Finally, the coordinates are sent through an RF channel to a central system for further processing.

These steps are shown visually in Fig. 7, where the conventional cross-correlation-based times and power consumption are compared with those of the proposed EML system.

The EML system has two main advantages: 1) the inference computation has a much lower computational cost and thus a much shorter duration of cross-correlation, allowing a higher positioning rate and energy savings compared to the conventional system; 2) in the conventional system, the hardware to receive the RF synchronization signal and then transmit the results consumes much more than the essentially passive RFID channel.

The direct comparison between cross-correlation techniques and EML positioning clearly indicates superiority in terms of positioning performance of the computation technique based on cross-correlation.

Nonetheless, some further interesting conclusions can be drawn from their comparison.

Although chirp is not the most suitable signal for recognizing signal maxima, the EML-based technique has proven robust in coordinate regression. The qualitative reconstruction of the trajectory is correct up to considerable levels of perturbation (jitter), enabling a substantial number of applications that do not require centimeter accuracy, as also demonstrated in Fig. 8, that fixes the limit to 25 cm. In the comparison, it should be considered that the microcontroller calculates the inference on-board in a time of about 10 ms, allowing a very high refresh rate of the positioning when compared to the results of a few Hertz shown in [17].

Furthermore, the memory requirements of the embedded device are severely reduced by this approach since it is necessary to memorize only the indexes of the signal peaks. The reduced requirements in terms of memory and computation allow imagining an application of this kind realized on a battery-less device that uses energy harvesting for its power supply [31]. Emerging applications where the accuracy of 25 cm is sufficient are, among others, navigation in indoor environments such as shopping centers, hospitals, airports, asset tracking in hospitals or factories, positioning of parcel storage for logistics, etc.

IV. Conclusion

In this paper, a novel system for indoor positioning based on RFID standard polling features, which exploits on-board feature selection and direct multi-output regression inference through EML techniques, is presented.

Previously assessed experimental tests on the time uncertainty of the synchronization procedure with the use of standard RFID tags and readers have been used for demonstrating the improvement in terms of inference time, and memory and computation requirement when using a neural network on a microcontroller for positioning measurements. The system has been proven able to provide positioning accuracy of 25 cm in the 95% of the positionings in the worst case, and a high-rate trajectory reconstruction thanks to an on-board inference time of about 10 ms. The reduced requirements in terms of memory and computation here obtained allow to envision three-dimensional ultrasonic positioning carried out by a device power supplied by energy harvesting. This paves the way for battery-less edge-AI powered services such as indoor navigation, asset tracking, home automation, and Internet of Things applications. In future works, authors will prospect the use of different ML models to increase the overall system's accuracy and will introduce transfer learning to improve system scalability without conducting additional site survey or compromising accuracy when labeled data is lacking.

References

[1] G. M. Mendoza-Silva, J. Torres-Sospedra, and J. Huerta, "A meta-review of indoor positioning systems," *Sensors*, vol. 19, no. 20, p. 4507, 2019, doi: 10.3390/s19204507.

[2] F. Zafari, A. Gkelias, and K. K. Leung, "A survey of indoor localization systems and technologies," *IEEE Commun. Surveys Tuts.*, vol. 21, no. 3, pp. 2568–2599, 3rd Quart., 2019, doi: 10.1109/COMST.2019.2911558.

[3] C. T. Nguyen *et al.*, "A comprehensive survey of enabling and emerging technologies for social distancing—Part I: Fundamentals and enabling technologies," *IEEE Access*, vol. 8, pp. 153479–153507, 2020, doi: 10.1109/ACCESS.2020.3018140.

[4] D. Zhang, F. Xia, Z. Yang, L. Yao, and W. Zhao, "Localization technologies for indoor human tracking," in *Proc. 5th Int. Conf. Future Inf. Technol.*, 2010, pp. 1–6, doi: 10.1109/FUTURETECH.2010.5482731.

[5] R. J. Przybyla, H.-Y. Tang, S. E. Shelton, D. A. Horsley, and B. E. Boser, "12.1 3D ultrasonic gesture recognition," in *Dig. Tech. Papers IEEE Int. Solid-State Circuits Conf.*, vol. 57, 2014, pp. 210–211, doi: 10.1109/ISSCC.2014.6757403.

[6] R. Carotenuto and P. Tripodi, "Touchless 3D gestural interface using coded ultrasounds," in *Proc. IEEE Int. Ultrason. Symp. (IUS)*, 2012, pp. 146–149, doi: 10.1109/ULTSYM.2012.0036.

[7] H. T. Kasprzak and D. R. Iskander, "Ultrasonic measurement of fine head movements in a standard ophthalmic headrest," *IEEE Trans. Instrum. Meas.*, vol. 59, no. 1, pp. 164–170, Jan. 2010, doi: 10.1109/TIM.2009.2022431.
[8] M. Merenda, G. Cimino, R. Carotenuto, F. G. D. Corte, and D. Iero, "Device-free hand gesture recognition exploiting machine learning applied to RFID," in *Proc. 6th Int. Conf. Smart Sustain. Technol. (SpliTech)*, 2021, pp. 1–5, doi: 10.23919/SpliTech52315.2021.9566385.
[9] N. El-Sheimy and Y. Li, "Indoor navigation: State of the art and future trends," *Satellite Navig.*, vol. 2, no. 1, p. 7, 2021, doi: 10.1186/s43020-021-00041-3.
[10] A. Nessa, B. Adhikari, F. Hussain, and X. N. Fernando, "A survey of machine learning for indoor positioning," *IEEE Access*, vol. 8, pp. 214945–214965, 2020, doi: 10.1109/ACCESS.2020.3039271.
[11] G. D. Voinea, S. Butnariu, and G. Mogan, "Measurement and geometric modelling of human spine posture for medical rehabilitation purposes using a wearable monitoring system based on inertial sensors," *Sensors*, vol. 17, no. 1, p. 3, 2017, doi: 10.3390/s17010003.
[12] R. A. Cooper *et al.*, "A perspective on intelligent devices and environments in medical rehabilitation," *Med. Eng. Phys.*, vol. 30, no. 10, pp. 1387–1398, 2008, doi: 10.1016/j.medengphy.2008.09.003.
[13] A. Marco, R. Casas, J. Falco, H. Gracia, J. I. Artigas, and A. Roy, "Location-based services for elderly and disabled people," *Comput. Commun.*, vol. 31, no. 6, pp. 1055–1066, 2008, doi: 10.1016/j.comcom.2007.12.031.
[14] M. Merenda, D. Iero, R. Carotenuto, and F. G. D. Corte, "Simple and low-cost photovoltaic module emulator," *Electronics*, vol. 8, no. 12, p. 1445, 2019, doi: 10.3390/electronics8121445.
[15] M.-H. Kang and B.-G. Lim, "An ultrasonic positioning system for an assembly-work guide," *J. Signal Process. Syst.*, vol. 93, no. 9, pp. 1045–1056, 2021, doi: 10.1007/s11265-021-01672-0.
[16] A. Iula, "Ultrasound systems for biometric recognition," *Sensors*, vol. 19, no. 10, p. 2317, 2019, doi: 10.3390/s19102317.
[17] R. Carotenuto, M. Merenda, D. Iero, and F. G. D. Corte, "An indoor ultrasonic system for autonomous 3-D positioning," *IEEE Trans. Instrum. Meas.*, vol. 68, no. 7, pp. 2507–2518, Jul. 2019, doi: 10.1109/TIM.2018.2866358.
[18] F. Ijaz, H. K. Yang, A. W. Ahmad, and C. Lee, "Indoor positioning: A review of indoor ultrasonic positioning systems," in *Proc. Int. Conf. Adv. Commun. Technol. (ICACT)*, 2013, pp. 1146–1150.
[19] M. T. Chew, F. Alam, M. Legg, and G. S. Gupta, "Accurate ultrasound indoor localization using spring-relaxation technique," *Electronics*, vol. 10, no. 11, p. 1290, 2021, doi: 10.3390/electronics10111290.
[20] M. Saad, C. J. Bleakley, T. Ballal, and S. Dobson, "High-accuracy reference-free ultrasonic location estimation," *IEEE Trans. Instrum. Meas.*, vol. 61, no. 6, pp. 1561–1570, Jun. 2012.
[21] R. Carotenuto, M. Merenda, D. Iero, and F. G. D. Corte, "Mobile synchronization recovery for ultrasonic indoor positioning," *Sensors*, vol. 20, no. 3, p. 702, 2020, doi: 10.3390/s20030702.
[22] M. M. Saad, C. J. Bleakley, and S. Dobson, "Robust high-accuracy ultrasonic range measurement system," *IEEE Trans. Instrum. Meas.*, vol. 60, no. 10, pp. 3334–3341, Oct. 2011, doi: 10.1109/TIM.2011.2128950.
[23] L. Mainetti, L. Patrono, and I. Sergi, "A survey on indoor positioning systems," in *Proc. 22nd Int. Conf. Softw. Telecommun. Comput. Netw. (SoftCOM)*, 2014, pp. 111–120, doi: 10.1109/SOFTCOM.2014.7039067.
[24] R. Carotenuto, M. Merenda, D. Iero, and F. G. D. Corte, "Ranging RFID tags with ultrasound," *IEEE Sensors J.*, vol. 18, no. 7, pp. 2967–2975, Apr. 2018, doi: 10.1109/JSEN.2018.2806564.
[25] R. Carotenuto, M. Merenda, D. Iero, and F. G. D. Corte, "Simulating signal aberration and ranging error for ultrasonic indoor positioning," *Sensors*, vol. 20, no. 12, pp. 1–14, 2020, doi: 10.3390/s20123548.
[26] M. Merenda, L. Catarinucci, R. Colella, F. G. D. Corte, and R. Carotenuto, "Exploiting RFID technology for indoor positioning," in *Proc. 6th Int. Conf. Smart Sustain. Technol. (SpliTech)*, 2021, pp. 1–5, doi: 10.23919/SpliTech52315.2021.9566443.
[27] R. Carotenuto, M. Merenda, D. Iero, and F. G. D. Corte, "Using ANT communications for node synchronization and timing in a wireless ultrasonic ranging system," *IEEE Sens. Lett.*, vol. 1, no. 6, pp. 1–4, Dec. 2017, doi: 10.1109/lsens.2017.2776136.
[28] "SensComp Series 7000." [Online] Available: https://senscomp.com/wp-content/uploads/2019/12/V2_Series-7000-Ultrasonic-Sensor-Spec-31July14.pdf (Accessed: May 10, 2022).
[29] D. Kocev, S. Džeroski, M. D. White, G. R. Newell, and P. Griffioen, "Using single- and multi-target regression trees and ensembles to model a compound index of vegetation condition," *Ecol. Model.*, vol. 220, no. 8, pp. 1159–1168, Apr. 2009, doi: 10.1016/J.ECOLMODEL.2009.01.037.
[30] "EM4325." [Online]. Available: https://www.emmicroelectronic.com/sites/default/files/products/datasheets/4325-ds_0.pdf (Accessed: May 10, 2022).
[31] M. Merenda, S. Pizzi, R. Carotenuto, A. Molinaro, F. D. Corte, and A. Iera, "Design principles of a fully-passive RFID-based IoT sensing node," in *Proc. 24th Eur. Wireless Futures Era Netw. Programmability (EW)*, 2018, pp. 162–167.

Massimo Merenda (Member, IEEE) received the bachelor's, master's, and Ph.D. degrees in electronic engineering from the University "Mediterranea" of Reggio Calabria (UNIRC), Italy, in 2002, 2005, and 2009, respectively. From 2003 to 2005, he was a Fellow with the Institute of Microelectronics and Microsystems, National Research Council IMM-CNR, Naples, Italy. From 2011 to 2018, he was a Postdoctoral Researcher with UNIRC. He was a Researcher with the DIIES Department, UNIRC, and CNIT, from 2018 to 2021. He is currently a Senior Scientist with the Cooperative Digital Technologies Competence Unit, Austrian Institute of Technology, Vienna. He is a member of the AIOTI alliance and of the COST action CA20120 INTERACT. His research activity is mainly focused on the design of CMOS IC, silicon sensors, energy harvesting, RFID smart tag and applications, embedded systems, Internet of Things, edge computing for applications of the Internet of Conscious Things and beyond.

Luca Catarinucci (Senior Member, IEEE) is an Associate Professor of Electromagnetic Fields with the Department of Innovation Engineering, University of Salento, Lecce, Italy, where he teaches Microwaves and Electromagnetic Solutions for Hi-Tech. Besides various activities in the classical areas of Electromagnetics, in 2005 he begun a new research tread referred to radiofrequency identification systems (RFID), dealing with reader and tag antenna design, realization of microwave circuits for the integration of UHF RFID Systems with sensor networks, design of automatic platforms for the over-the-air performance evaluation of RFID tags, prototyping of fully passive RFID tags provided with computational and sensing capabilities, study of new antennas for handheld RFID readers, joint use of 3D-printed electronics and RFID, and introduction of Doppler-based RFID-inspired backscattering modulation. He is currently the Vice President of Technical Activities at the IEEE Council of RFID (CRFID). He authored more than 200 scientific works of which 83 on international journals, four chapters of books with international diffusion and more than 89 proceedings of international conferences. Moreover, he holds two National Patents about RFID technology.

Riccardo Colella (Senior Member, IEEE) received the M.Sc. degree (Hons.) in telecommunication engineering and the Ph.D. degree from the University of Salento, Italy, in 2010 and 2015, respectively. He is a Researcher of Electromagnetic Fields Area with the Department of Innovation Engineering, University of Salento. He authored about 140 papers appeared on international journals and in national and international conferences, two book chapters with international diffusion, and a patent. His research activity is mainly focused on the design of innovative RFID antennas, wirelessly-powered IoT sensing systems, antennas for healthcare applications, and novel RF electronics devices and antennas in 3D-printing technology.

Demetrio Iero received the master's degree in electronic engineering from the University "Mediterranea" of Reggio Calabria, Reggio Calabria, Italy, in 2010, and the Ph.D. degree in 2014. He is currently a Researcher with the DIIES Department, University "Mediterranea" of Reggio Calabria. His main research activities include power electronics and converters, power loss measurement techniques, microcontrollers and embedded systems, IoT, and RFID platforms.

Francesco G. Della Corte (Senior Member, IEEE) received the Laurea degree in electronic engineering from the University of Napoli, Naples, Italy, in 1988. He is currently a Full Professor of Electronics with the University Federico II of Naples, Italy. His current research interests include wide bandgap semiconductor device modeling for high temperature and high power applications, silicon photonics, and wireless smart sensors.

Riccardo Carotenuto (Senior Member, IEEE) was born in Rome, Italy. He received the Dr.Sc. degree in electronic engineering and the Ph.D. degree from the University "La Sapienza" of Rome, Rome, Italy. He has been an Associate Professor of Electronics with the University "Mediterranea" of Reggio Calabria, Reggio Calabria Italy, since 2002. He authored or coauthored more than 120 papers published in international journals and conferences proceedings. His main interests include power conversion, energy harvesting, indoor localization, ultrasound imaging, ultrasound actuators, and neural networks theory and applications.